Source Term and Containment Issues Paper N°3.6

Understanding the behaviour of absorber elements in silver-indium-cadmium control rods during PWR severe accident sequences

R. Dubourg[2], H. Austregesilo[1], C.Bals[1], M.Barrachin[2], J.Birchley, T.Haste[3], I.Nagy[4], J.S.Lamy[5], T.Lind[3], B.Maliverney[5], C. Marchetto[2], A.Pinter[4], M. Steinbrück[6], J.Stuckert[6], K.Trambauer[1] and A.Vimi[4].

CONTRACT SARNET FI6O-CT-2004-509065

1) GRS, Garching (G)
2) IRSN DPAM/SEMIC, Cadarache (Fr)
3) PSI, Villigen (CH)
4) AEKI, Budapest (Hun)
5) EDF R&D, Clamart (Fr)
6) FZK, Karlsruhe (G)

Summary

In the case of a hypothetical severe accident in a Pressurized Water Reactor (PWR), Silver-Indium-Cadmium (SIC) control rod failure occurs early during the sequence. Release of absorber elements could induce early fuel rod degradation by interaction of molten SIC alloy with fuel rod cladding, and the absorber materials could interact with the fission products, affecting significantly their speciation and transport in the primary circuit as well as their behaviour in the containment. This paper summarises the experimental and modelling progress made on this topic within SARNET over the whole project.

Following a review of the status of knowledge, including the modelling in the main codes (ATHLET-CD, MAAP4, SCDAP, MELCOR, ASTEC), detailed calculations of the analytical EMAIC and integral Phebus FPT2 experiments were performed. Accurate calculation of vapour pressure of the molten absorber elements is needed, requiring reliable values of the activity coefficients. The importance of accurate reproduction of the control rod degradation was shown, with the behaviour of absorber elements at rupture being critical as well as the thermodynamic data and speciation of the system Ag-In-Cd-Zr-H-O.

The QUENCH-13 bundle experiment (FZK) in realistic integral geometry, with 20 electrical heated rod simulators and one central SIC rod, has helped to characterise the behaviour of absorber elements at the time of rod rupture, with measurements of the SIC release, using impactors (AEKI) and electrical low-pressure impactor and Berner low-pressure impactors (PSI). Coordinated pre and post test calculations using SCDAP-based codes (PSI), MAAP4 (EdF), ATHLET-CD (GRS), ASTEC (IRSN) helped in defining the test and beginning of its interpretation. It was supported by separate-effects tests on short control rod segments (FZK); 5 were performed to aid in the main test definition, with 5 reserved for later interpretation; the tests showed different failure mechanisms at temperatures always over 1473 K. In QUENCH-13 the on-line aerosol measurements with electrical low-pressure impactors indicated control rod failure in the range 1550-1600 K; the test was terminated later at 1813 K by water reflood. Analysis of aerosol measurement results showed significant Cd and In release after rod failure with lower release of Ag. Relocated SIC melt in the form of rivulets was detected in the lower part of the bundle. Investigation of SIC material properties (solidus, liquidus) by further analysis of data from QUENCH-13 is also presented.

In parallel, an exhaustive review of activity coefficients of the elements in the SIC melt, including the effect of Zr was began (IRSN with the CNRS of Marseille), also, from CORA, and from new separate-effects tests at FZK.

A. INTRODUCTION

Vaporization of metallic elements from the Ag–In–Cd control rods in light-water reactors under accident conditions, the amount released and the nature of the species transported are important for the studies relating to the severe accidents for the following reasons. First, except may be for uranium, the silver and indium release is the main contributor in terms of mass to the aerosols present along the Reactor Coolant System (RCS). Thus, it may affect the aerosol deposition modeling via the density and the size of the aerosols formed. Secondly, silver and indium are very reactive with iodine which is a major contributor to the source term to environment, at least at short time. Kinetic release and the chemical composition through the RCS of these elements are of prime importance in order to evaluate the gaseous fraction of iodine reaching the containment. It is indeed suspected from the PHEBUS- FPT0, FPT1 [1] that the gaseous fraction of iodine measured experimentally could be due to some kinetic limitations [2], as all calculations based on assumption that gaseous compounds are always in chemical equilibrium could not predict this fraction probably because silver, coming from sedimentation, reacts with iodine to trap it very quickly. The kinetics and the extent of the irreversible trapping depend on the nature (oxidized form or not) and the amount of silver dissolved in the sump. For the three reasons mentioned here above, all data, which permit to better characterize the absorber elements volatility, are useful to improve the modeling of the fission products release outside the containment. The literature relevant to the release of Ag, In, and Cd from control rods under reactor accident conditions has been reviewed by Petti [3, 4].

There is a general knowledge on the control rod behaviour and absorber elements release during an accident sequence coming from numerous previous analytical experiments (SASCHA [5], Winfrith [6, 7]; semi-analytical experiments (EMAIC [8] or more integral experiments (CORA [9], FALCON, [10], PBF-SFD [11], PHEBUS [1]). The main results and findings from these experiments were presented earlier in the frame of SARNET work [12]. In this review it was shown also that the models implemented in many codes took already into account much of this knowledge. Nevertheless, benchmarking of these codes against EMAIC or PHEBUS FPT1 and FPT2 tests [13] revealed a number of points needing improvements and better knowledge.

The main uncertainty concerned the behaviour of the absorber elements at the time of the rod rupture. In the case of early small rupture (by low melting point eutectics formation), an instantaneous release of a part of the cadmium vapours formed inside the rod prior the rupture might be foreseen. In addition, a part of the remaining SIC molten alloy at the elevation of the rupture could be forcibly ejected by spraying inducing possible interactions with surrounding fuel elements and beginning of their degradation.

For the release after significant rod rupture, both calculations [14] and experimental results [8] indicate that cadmium is by far the most volatile of the three elements. The vaporization of silver appears to be relatively simple, and is dominated by the monatomic gas-phase species, Ag (g), with only minor contributions from Ag_2 (g) and AgO (g). The possible importance of AgOH (g) and AgH (g), which are not included in the thermochemical databases, was not evaluated. In contrast with silver, the vaporization of indium is complicated by reactions with steam to form In_2O (g), InOH (g), and In_2O_3(s) (especially under oxidizing conditions). Reaction of steam with the (Ag, In) alloy to form (Ag, In, O) introduces an additional degree of freedom to the vaporization equilibriums. Interactions

between the alloy and zirconium or iron do not appear to impact strongly on the vaporization, unless the alloy is diluted by large amounts of zirconium.

In fact, uncertainties on the activity coefficient of the elements are very important remaining items to consider for deriving reliable expressions for vapor pressures of absorber elements.

Regarding these points of uncertainties it was decided to promote two types of additional investigations. Firstly, definition and realization of the QUENCH-13 test designed in rather realistic geometry and instrumented for accurate evaluation and characterization of aerosols release during control rod degradation and at time of rod rupture. In addition to the QUENCH-13 experiment, analytical experiments with small samples of different designs and heating modes were performed to investigate the behavior of control rod at the rupture. The test conditions were defined on the basis of extensive planning analyses by PSI, GRS and EDF [15].

Secondly, the experiments are complemented by an exhaustive review of the thermodynamic properties of Ag-In-Cd-O-H-Zr system that is being performed.

The first results obtained on these recent actions are presented in this paper.

B. THE QUENCH 13 EXPERIMENT

B.1 Description of the test facility and of the test sequence

The QUENCH-13 test was performed at the Forschungszentrum Karlsruhe on 7 November, 2007. The QUENCH facility is constructed to investigate the hydrogen source term resulting from the water injection into an uncovered core of a Light-Water Reactor as well as the high-temperature behavior of core materials under transient conditions. The typical QUENCH test bundle consists of 21 fuel rod simulators with a total length of approximately 2.5 m. The heating is electric with 1 m length tungsten heaters inside fuel rod simulators. The cladding material of rod simulators is standard Zircaloy-4. Fuel is represented by the ZrO_2 pellets. During the test, some of corner rods, inserted in the bundle to simulate the real gas channel conditions could be withdrawn. The bundle is extensively instrumented with about 60 thermocouples distributed along 17 axial positions. In the QUENCH-13 test, the single unheated fuel rod simulator in the centre of the normal 21-rod fuel bundle was replaced by a PWR control rod (fig. 1).

The QUENCH-13 experiment investigated the effect of this control rod on early-phase bundle degradation, i.e. AgInCd/stainless steel/Zircaloy-4 control rod materials on oxidation and melt formation, and on reflood behavior [16]. The test comprised pre-oxidation at temperature below the rod rupture, then slow ramp temperature transient defined for accurate observations around the rod rupture, and at last, quench water injection at the bottom of the test section (fig. 2).

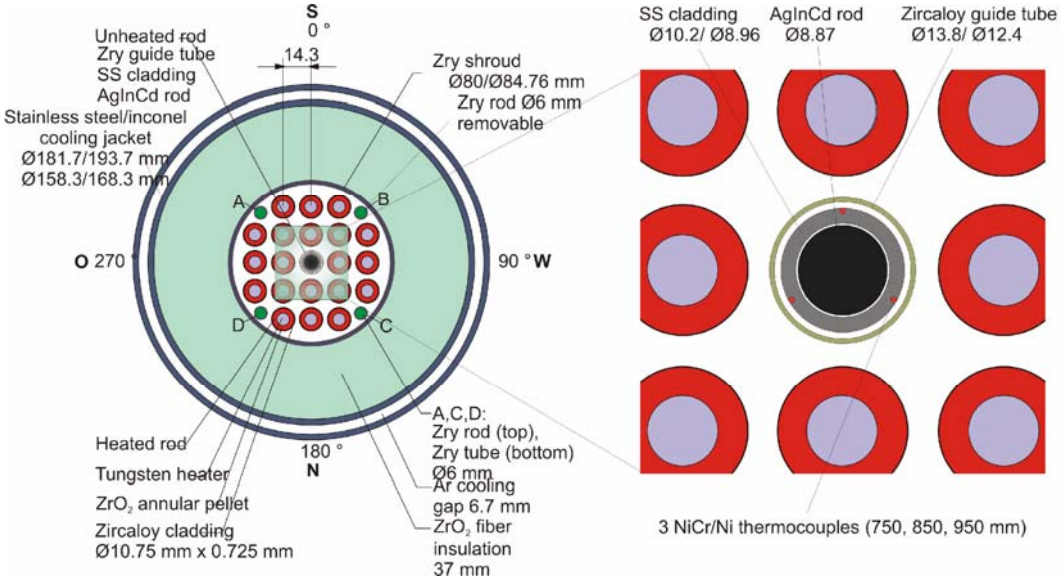

Figure1 : QUENCH-13 fuel rod simulator bundle (cross section)

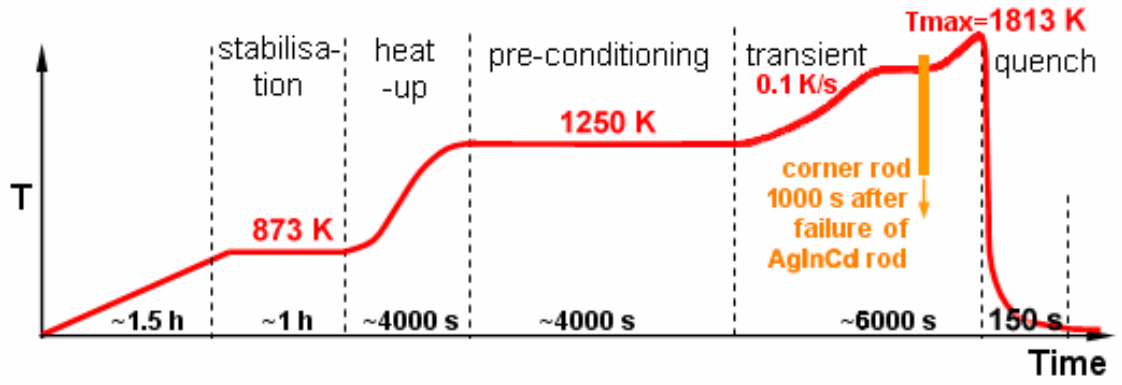

Figure 2: QUENCH-13 test conduct (temperature profile on hottest elevation of 950 mm).

B.2 Control rod behaviour and analysis of relocated materials

The solidus of Ag-In-Cd is identified at ~1000 K and the liquidus at 1100 K. The failure of control rod with melt release and first aerosol detection is observed between 1550 and 1620 K at hottest bundle elevation of 950 mm. A significant melt release is observed by 1650 K (at 950 mm) during temporary transient interruption and perhaps massive melt relocation by 1650 K (at 950 mm) during continuation of transient (fig.3). The failure of control rod at elevation 950 mm was later confirmed by metallographic investigation of the corresponding bundle cross-section [17].

The post-test visual investigation of bundle structures with endoscope revealed the solidification of relocated melt at elevations between third and first spacer grids (SG3 and SG1 respectively) (fig.4).

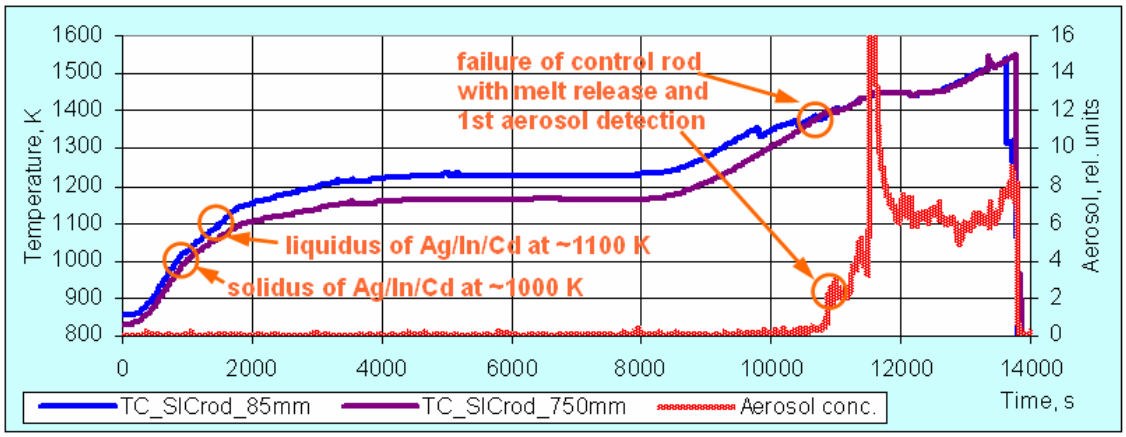

Figure 3: QUENCH-13 sequence of events

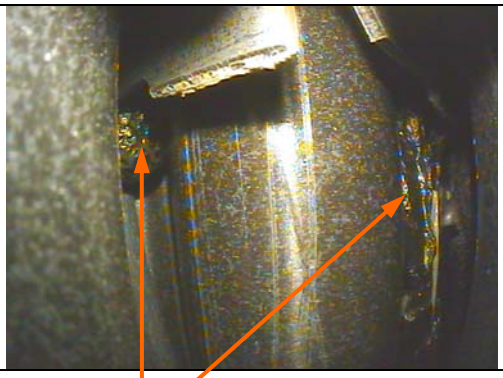

550 mm, AIC melt at lower edge of SG 3

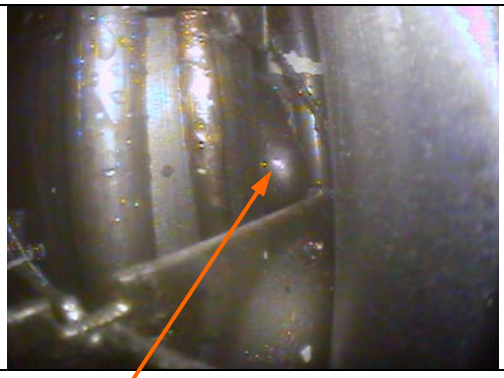

-50 mm, AIC melt at upper edge of SG1

Figure 4 : QUENCH-13, videoscope: Ag/In/Cd melt relocation into lower part of the bundle

An EDX analysis of the relocated melt was performed at elevations 550 mm and 34 mm. Typical structures of investigated melt, relocated outside of the control rod, is pictured in figure 5. Points in this figure marked locations of the EDX measurements. Corresponding measurement results are collected in table 1.

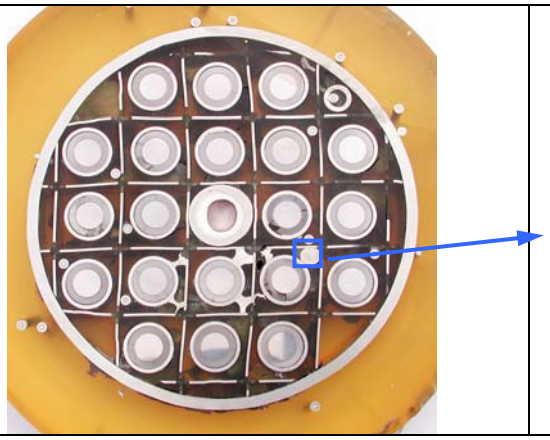

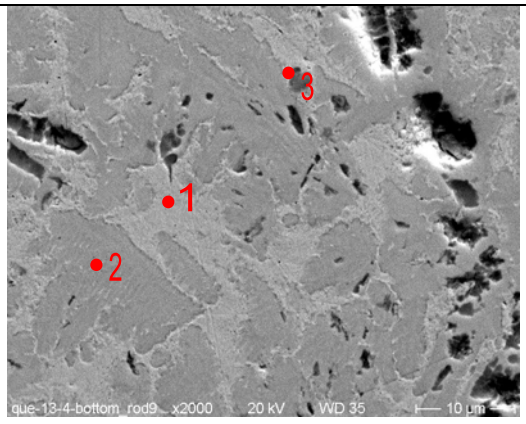

Figure 5 : Bundle cross-section at elevation 550 mm (left) and structure of frozen melt relocated after CR failure to elevation 550 mm. (right).

	Ag	In	Cd	Zr	Fe	Cr	Ni	O	area ratio, %
1	87	4	8	1					20
2	39	12	0.5	45	3		0.4		79.5
3	10	4	1	37	28	11	1	8	0.5

Table 1: Elemental composition (wt%) of typical components of frozen melt at 550 mm

The EDX analysis of relocated melt shows a very significant amount of Ag and significantly higher content of dissolved zirconium in comparison to dissolved stainless steel fractions.

B.3 Aerosols measurements during the QUENCH-13 experiment

To characterize the extent of aerosol release during the control rod failure, aerosol particle size distribution and concentration measurements in the off-gas pipe of the QUENCH facility were carried out. For the first time, it was possible to determine on-line the aerosol concentration released from the core. This enabled the determination of the exact time of the control rod failure, as well as gave an indication of the control rod failure mechanism. In addition, samples were collected for elemental analysis to define the elemental composition of the released aerosol at two different times after the control rod failure. The aerosols were sampled from QUENCH facility off-gas pipe at the gas temperature of approximately 300°C and at the pressure of 2.0 bar (abs).

PSI used 2 types of aerosol measurement instruments:

- Electrical low-pressure impactor (ELPI) size-classifies particles according to their aerodynamic mobility into 12 size classes, or stages, in the particle size range 0.03 – 10 µm. The particles entering the device are charged in a corona charger to a known equilibrium charge distribution, and the current caused by the depositing particles on consecutive stages is measured with sensitive electrometers.
- Berner low-pressure impactor (BLPI) is a cascade impactor that size-classifies particles according to their aerodynamic mobility to 12 mobility fractions [18].

AEKI installed also two types of aerosol collecting devices similar to the ones used in earlier CODEX experiments [19] and in the QUENCH-10 and 11 tests:

- Impactor system with ten impactors, each of them operated for about 1 minute at the most important steps of the test (e.g. before and after control rod failure, quenching), and
- Ni plate placed in the off-gas pipe of the QUENCH facility, which collected aerosol during the whole experiment.

The on-line measurement with ELPI (PSI) showed that the main aerosol release started at 10820s. A very large burst of aerosols was detected at 11480s, followed by a relatively steady aerosol release until quench when the on-line measurements were stopped.

The main particle mode after the control rod failure was found in the particle size range 0.1 – 3 µm. According to the EDX analysis, particles contained mainly Cd, In, W, and Ag. As these elements or their oxides are known to be volatile in the temperatures of the QUENCH test, we believe that during heat-up of the core they were released to the gas phase where they formed new particles by nucleation and condensation. Then the particles grew further by condensation of gas phase species onto their surface, and by agglomeration. According to SEM analyses of samples collected by AEKI, particle aggregates can have larger sizes up to 20-25 µm. Figure 6 shows aerosol particles collected at the beginning of control rod failure

(AEKI I3) and during cooling (AEKI I8). Almost homogeneous, Cd-oxide particles with rounded shape are characteristic for sample AEKI I3, while the size and the elemental composition varied among different particles deposited e.g. on sample AEKI I8.

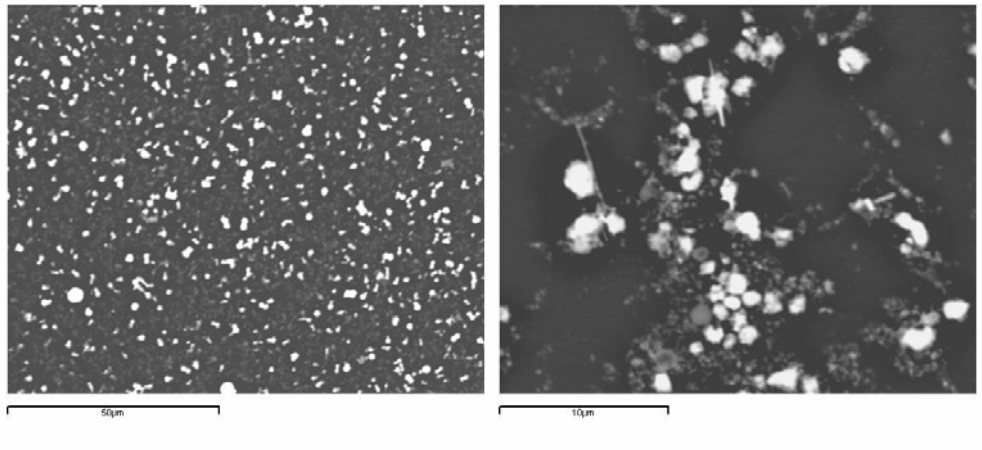

Figure 6: SEM images for two aerosol samples AEKI I3 (left) and I8 (right).

Summarized analytical data for aerosols taken by AEKI and PSI can be seen in figure 7.

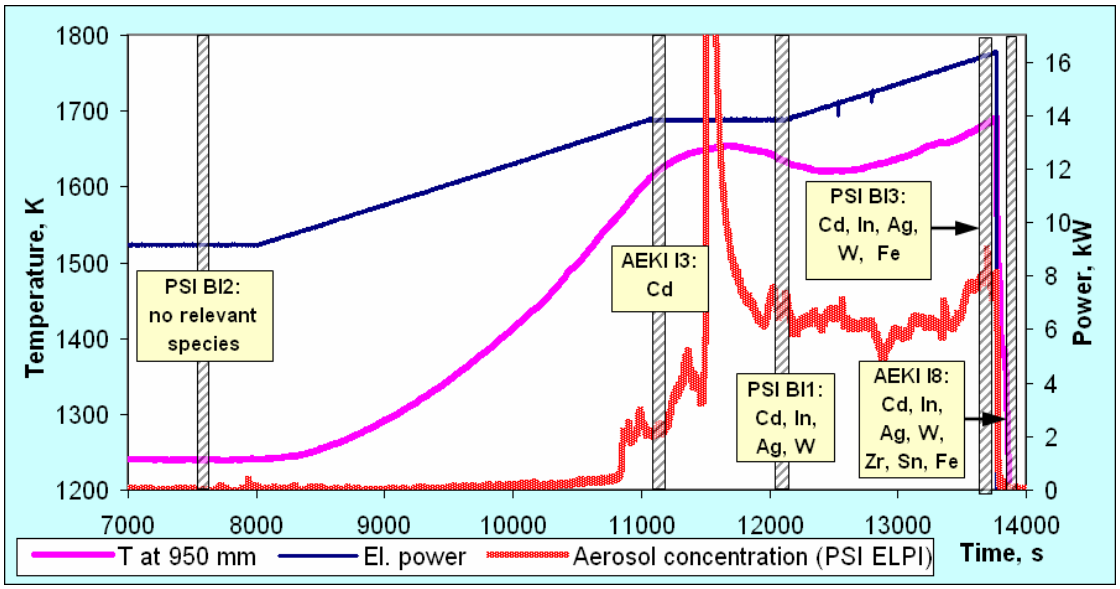

Figure 7: Analysis of aerosol release with PSI and AEKI impactors as well as on-line aerosol concentration measurements by ELPI.

The elemental composition from EDX analyses of particles collected by AEKI is shown in table 2.

Among the elements of the SIC rod first Cd (up to about 60 wt %) was found in sample taken at SIC failure (AEKI I3). In, W, Ag and Zr were first detected directly after SIC rod failure (AEKI I4). Maximum amounts of In were found at AEKI I4, for Ag after SIC failure (AEKI I6) and for Zr during quenching. It was found that Cd, In, W and Zr were detected more frequently than Ag (Table 2).

Sample	O	Cd	In	W	Ag	Zr	Sn	Fe	Mo
AEKI I3 (11097s)*	34	55.3	0	0	0	0	**	0	0
AEKI I4 (12070s)	26	18.2	35.7	14.4	**	**	**	0	0
AEKI I6 (13620s)***	7.6	0	2.1	6.9	29.4	0	3	1.9	0
AEKI I8 (13746s)	16.2	1.5	1.5	4.3	0	39.4	1.8	1.3	1
AEKI I8****	15.5	5.6	12.5	13.1	1	3.6	8	1.7	3
AEKI Ni	30.9	15	14.7	9.4	0.7	18.3	4.9	1.7	3.1

Table 2: Average quantitative EDX data for some aerosol samples (AEKI)

*Notes: *: Missing elements from the composition of AEKI I3 are impurity of average amounts: Si: 1.8 wt%, Cu: 4 wt%, Zn: 3.2 wt%.*

***: Traces were detected in some particles.*

****: The amount missing to 100 % is originating from the Si holder. The compositions of various particles were often different and they were deposited mostly rarely on the collector plates.*

*****: There were 2 different particles, some highly enriched in Zr and others enriched mostly in In and W.*

The elemental composition from EDX analyses of particles collected by PSI Berner impactor stage 6 (Dp = 0.4 – 0.7µm) in samples BLPI1, shortly after the control rod failure at t = 12106s, and BLPI3, immediately before quench at t = 13680s are given in table 3. Both show also that at the rod rupture Cd is significantly released.

sample	Cd	In	Ag	W	Fe
PSI BI1	42	41	2.5	14.5	
PSI BI3	33	31	8	27	1

Table 3: Elemental composition of aerosols released after CR failure (BI1) and before reflood (BI3) (PSI)

B.4 QUENCH separate-effects control rod tests

The bundle test QUENCH-13 was supported by single rod tests performed in the QUENCH-SR rig which allows inductive heating of rod specimens till their failure. The test rig is coupled with a mass spectrometer; temperatures are controlled and measured by a two-colour pyrometer and additionally measured by a thermocouple attached to the surface of the rod segment. Two video systems were installed to observe the failure mode and melt release.

10-cm long specimens with different designs regarding contact between Stainless Steel (SS) and Zry-4 tubes (symmetric, asymmetric) as well as regarding possibility of inner Zry oxidation (with and w/o 4-mm holes in the Zry guide tube) were manufactured. The test conduct was as close as possible to the planned QUENCH-13 test protocol, i.e. including a 5000-s plateau at 977 and 1150 °C, respectively, followed by a slow transient phase (0.1 K/s) till failure of the specimen. All tests were performed in an oxidising steam-argon atmosphere.

Five (out of ten) tests have been performed so far. Test matrix and main results are summarised in table 4. The failure temperatures were always above 1200 °C with the highest ones measured at the symmetric specimens (no contact between SS and Zry-4). The temperatures measured by thermocouples additionally indicate a later failure of specimens with (possibility of) inner oxidation of the Zircaloy guide tube. No clear influence of pre-oxidation temperature was seen. The failure mechanisms were quite different between the specimens, from local failure with melt droplet splashing and rivulet relocation till explosive

destruction. At the specimens with holes in the guide tube (allowing inner oxidation), the melt relocated internally and was released through these holes.

Test	Sample	T_{pre-ox}, °C	$T_{failure}$, °C (Pyro/TC)	Failure mode
SIC-01	asymmetric without holes	977	1240/1235	failure at lower part of specimen with massive melt discharge
SIC-02	asymmetric without holes	1150	1270/1225	failure at middle part of specimen with droplets and rivulets
SIC-03	asymmetric with holes	977	1235/1280	melt release through lower holes for steam access
SIC-04	symmetric with holes	977	1290/1290	melt release through upper holes for steam access
SIC-05	symmetric without holes	977	1355/1355	explosion of specimen

Table 4**:** Test matrix and main results of single rod experiments on SIC failure

The post-test appearance of the specimens is well documented by photography (fig 8). The metallographic post-test examination is under way. First results show a huge number of different phases due to the interaction between SIC, SS, and Zry-4. Furthermore, even very narrow gaps (10 µm) between the Zry guide tube and the SS cladding were found to be filled with SIC melt. Videos of all tests are additionally available.

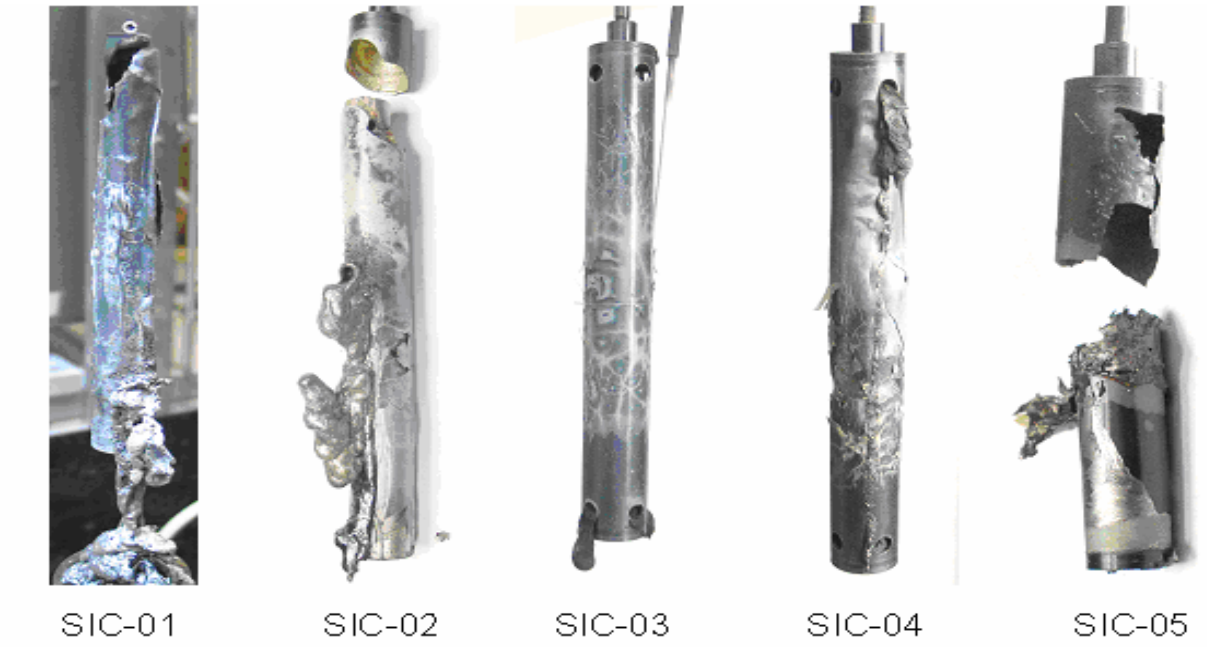

Figure 8: Post-test appearance of SIC single rod specimens

Experiments with the five remaining specimens are planned after analysis of the QUENCH-13 bundle test. Most probably, they will retrace the temperature histories of the elevations 950 mm (the hottest one) and 750 mm (lower failure position of the guide tube) of the bundle experiment.

B.5 Pre-test and preliminary post-test calculations of the QUENCH-13 experiment

Pre-test analytical support had been performed by PSI (with SCDAP), GRS (ATHLET-CD) and EDF (MAAP4) [15]. The models thus used provide the starting point for post-test analyses of the bundle heat-up, oxidation, SIC release and quenching.

The PSI pre-test model was modified to take account of the experimental boundary conditions in which power history was modified from the nominal specification to extend the time window between control rod failure and quench initiation. The base case calculation correctly followed the evolution until control rod failure. SCDAP uses a mechanistic model to calculate the interaction between the stainless steel cladding and the Zircaloy guide tube, and reproduced the time and temperature of this event with fair accuracy. The SIC relocation was qualitatively captured but the versions available currently at PSI do not extend to aerosol release and transport. The calculation did not capture the unexpected temporary decrease in both the temperatures at the hot elevation and in the hydrogen generation rate following control rod failure, resulting in an earlier calculated final escalation. Sensitivity calculations indicate that the main influence was a reduced oxidation heat. It is conjectured that the released SIC impinged onto the nearby cladding inhibited the oxidation, at lest temporarily. The calculated temperatures are compared in figure 9.

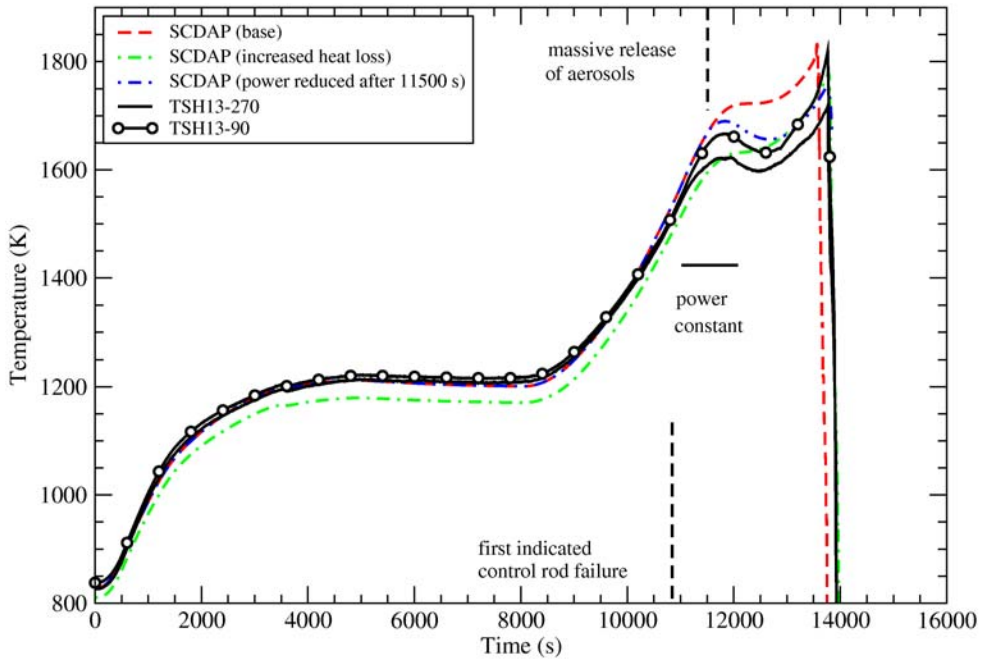

Figure 9: QUENCH 13 experimental data and calculated shroud temperature at 950 mm (SCDAP)

The hydrogen generation and SIC release characteristics are summarised in table 4. The analysis is currently at a preliminary stage, and will continue during the next year using models to examine the aerosol transport of SIC.

	SCDAP base	Increased heat loss in shroud	Power reduced by 500 W after 11500 s	Q-13 data
Time of control rod failure (s)	10250	10480	10250	10840
Temperature of control rod at time of failure (K)	1434	1435	1434	ca. 1415*
Mass of SIC relocated (g) - from elevation (mm) - to elevation (mm)	257 600 to 1024 100 to 300	257 600 to 1024 100 to 300	257 600 to 1024 100 to 300	 -150 to 550
Mass of H2 generated (g)	42	37	40	42
Quench initiation on - time (s) - peak shroud temperature (K)	temperature (13545) 1819	time 13763 (1774)	time 13763 (1814)	temperature 13766 1819

* control rod thermocouple affected by failure process; temperature estimated at ca. 1500 K based on thermal response elsewhere

Table 4: QUENCH-13 experiment and calculated signatures

The MAAP4 code has been used at EDF R&D to simulate the QUENCH-13 experiment.

The initial MAAP modeling shows large aerosol releases: cadmium is estimated to be fully released, indium at about 50 % and silver at about 5 % (fig 10: in black). The kinetics of cadmium and indium releases is obviously too fast. Improvements of the MAAP model have been implemented. The control rod rupture is now considered in the current node instead of the whole rod. This widely reduces the calculated releases of cadmium and indium. Besides, eutectics interaction between molten SIC and zirconium of the guide tube is introduced in the model. New results are shown on figure 10 (in red). The calculated cadmium and indium releases are respectively around 8 and 4 % while the silver release is now at 2.5%. Further improvements are planned using new thermodynamic data (cf. §C).

ASTEC code (V2dev version) post-test calculations were also performed. They gave reliable reproduction of the bundle temperature evolutions at different levels. At present no mechanistic models are available in the code for accurate reproduction of the control rod modes of rupture. A user defined criterion is used for this rupture, based on the stainless steel melting at 1723K. It gives poor reproduction of the time of rupture indicating that accurate modelling of Fe-Zr interactions (or at least a user-defined criterion based on temperatures deduced from separate-effects tests) are needed.

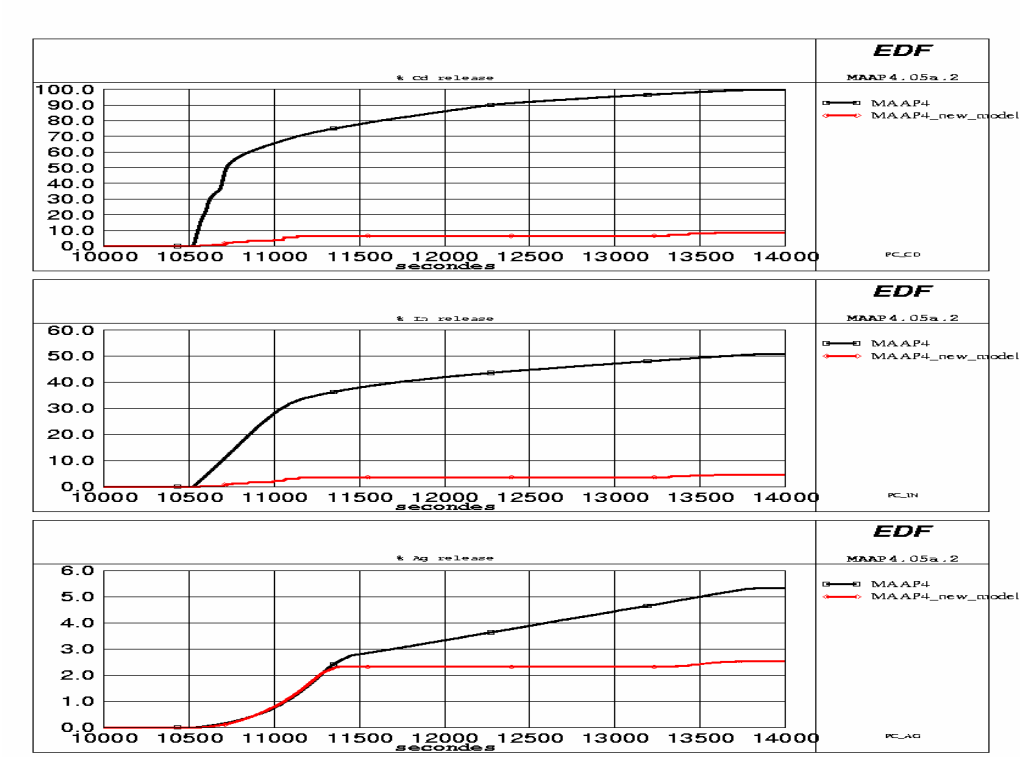

Figure 10: Cadmium, indium and silver releases from the QUENCH 13 bundle (%), calculated by MAAP4 code.

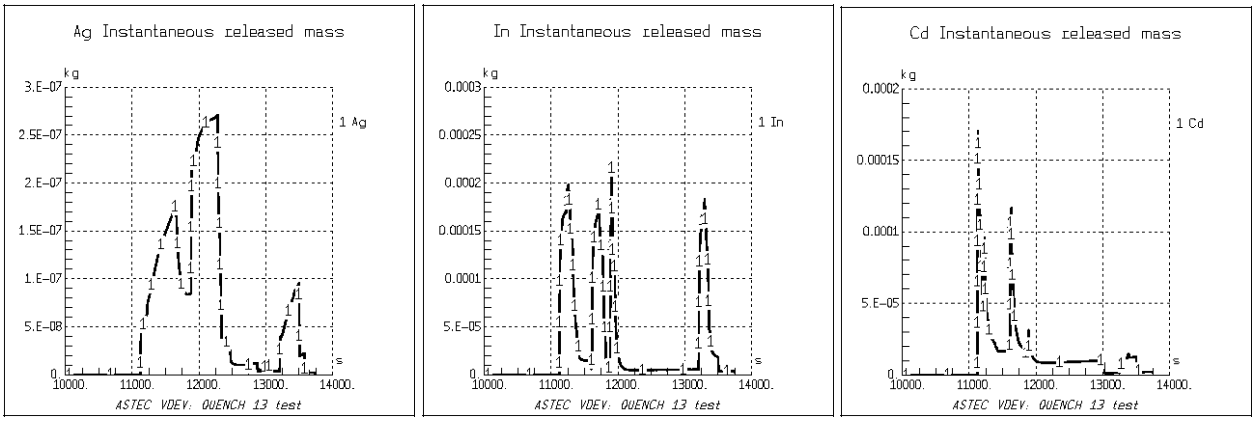

Figure 11: Instantaneous mass release in QUENCH13 calculated by ASTEC code for Ag, In, Cd.

Absorber elements releases calculated by theASTEC code are given in figure 11, expressed in instantaneous mass released for better comparison with table 2 and 3. Such comparison shows that the code reproduces rather well the main trends for Cd and In for example with aerosols mainly composed by Cd and In after the rod rupture and at the main aerosol release (fig7 and table 3). Nevertheless the burst release of only Cd (see AEKI I13 results) is not reproduced at the rod rupture (probably due to Cd already vaporised in the entire rod, prior its rupture). At present, such release is not considered in ASTEC code. Additionally, the Ag release, mainly during the late phases of the test sequence is underestimated, likely because of no reliable expression for its vapour pressure evolution, needing additional work on Ag speciation (see next paragraph).

Preliminary post-test calculations have been also performed with ATHLET-CD (fig 12). The results show a rather good agreement concerning the overall thermal behaviour, although hydrogen generation is slightly underestimated. About 150 g of absorber material is calculated to melt and relocate. With respect to SIC release, the results are qualitatively similar to those of the ASTEC code (Fig. 11), and confirm experimental findings concerning Cd burst release. As in the pre-test calculations [15], the code predicts only a rather small Ag release. Further in-depth analyses are planned as soon as the interpretation of experimental data is finished.

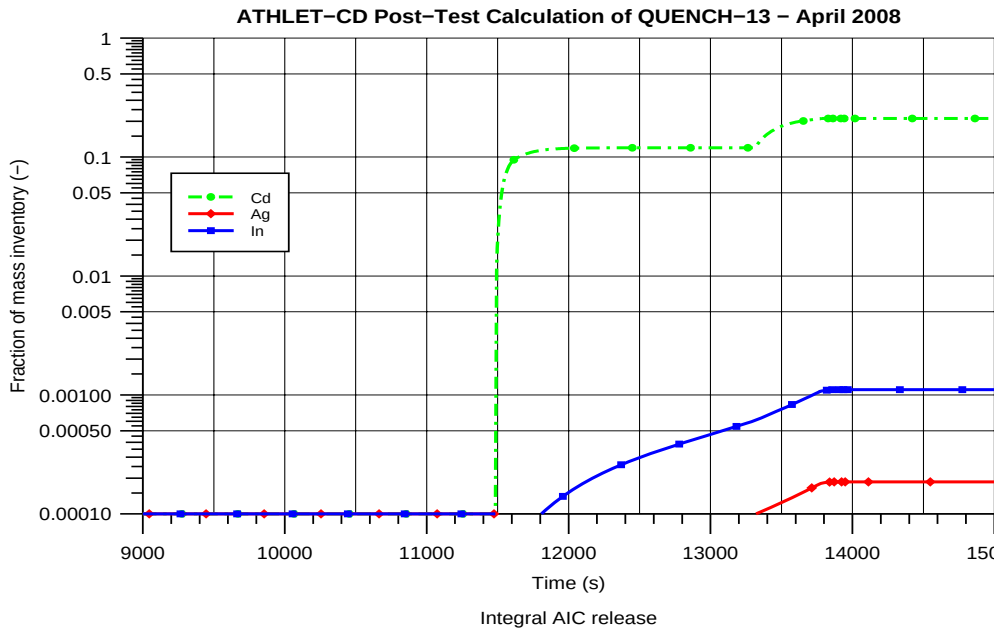

Figure 12: Integral SIC release from QUENCH-13 calculated by ATHLET-CD

C. REVIEW OF THERMODYNAMIC DATA OF THE SYSTEM AG-IN-CD-O-H-ZR

As mentioned in the introduction, the activity coefficients of the elements of the control rod are a very important item to consider in order to derive reliable expressions for vapor pressures of absorber elements. From a general point of view, the total vapour pressure over the SIC alloy is the sum of the partial pressures of each vapour species if the gas phase is taken to be ideal. The partial pressures depend on the concentration (X_i) of the different components (i) constituting the control rod material and the activity coefficients (γ_i) of these components in the liquid alloy. The relationship between the vapour pressure (p_i) of a component and its concentration in the alloy (X_i) is written as:

$$P_i = p_i^\circ \, \gamma_i \, X_i$$

where p_i° is the vapour pressure of i in the pure state.

In thermodynamic experiments, the activity (a_i) of a component is usually measured from its vapour pressure ($p_i = p_i^\circ \, a_i$), converting a_i to γ_i using the equation $a_i = \gamma_i \, X_i$. Another mean of evaluating the activity coefficients is the determination of heat of mixing (ΔH_m) of the alloy. In the strict case of a regular solution, there is a relationship between ΔH_m and the activity coefficients. For a ternary compound, this relation takes the following form :

$$\Delta H_m = RT\,(X_A\,Ln\,\gamma_A + X_B\,Ln\,\gamma_B + X_C\,Ln\,\gamma_C)$$

The review of the bibliography related to measurements of activity coefficients or enthalpies of mixing in the Ag-In-Cd ternary system and the different binary phase diagrams (Ag-In, Ag-Cd and In-Cd) was performed with the support of the TECSEN Laboratory of CNRS Marseille. The review of the different bibliographic data is reported in figures 13, 14 and 15. There are no data related to activity or mixing enthalpy in the ternary system Ag-In-Cd in the liquid state. The mixing enthalpies in the binary Ag-In and Ag-Cd phase diagrams indicate a negative deviation from ideal whereas the mixing enthalpy in Cd-In liquids is positive. Consequently it is expected to have some concentrations in the ternary phase diagram for which the Ag-In-Cd mixture ideally behaves. Determinations of activity or mixing enthalpy for compositions representative of the ternary alloys are envisaged to complete the experimental database and to allow the modelling of the Gibbs energy of the ternary alloys in the liquid state.
The present bibliographic work will continue with the higher order systems including zirconium (component of the guide tube) and gas constituents (hydrogen and oxygen).

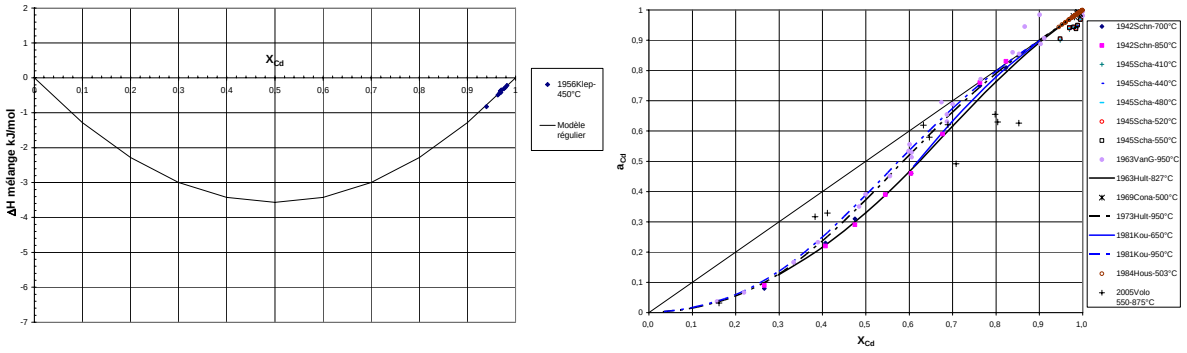

Figure 13: (a) Mixing enthalpy of Ag-Cd alloy, (b) Cd activity in liquid Ag-Cd

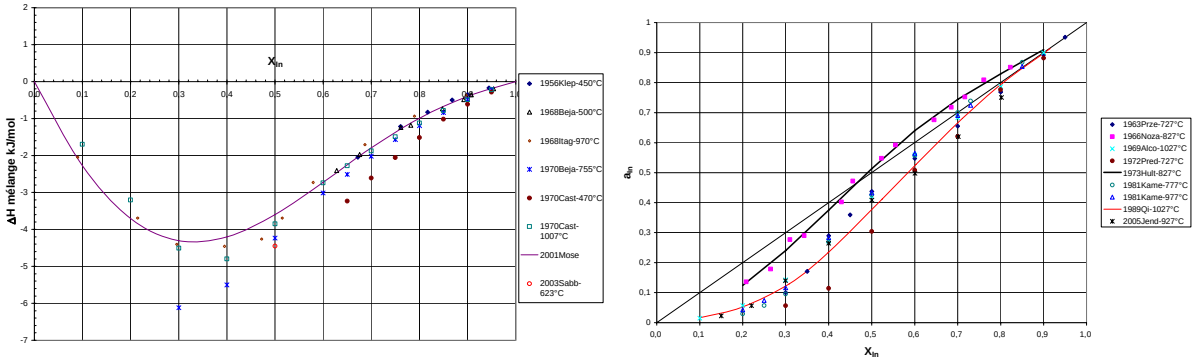

Figure 14: (a) Mixing enthalpy of Ag-In alloy, (b) In activity in liquid Ag-In

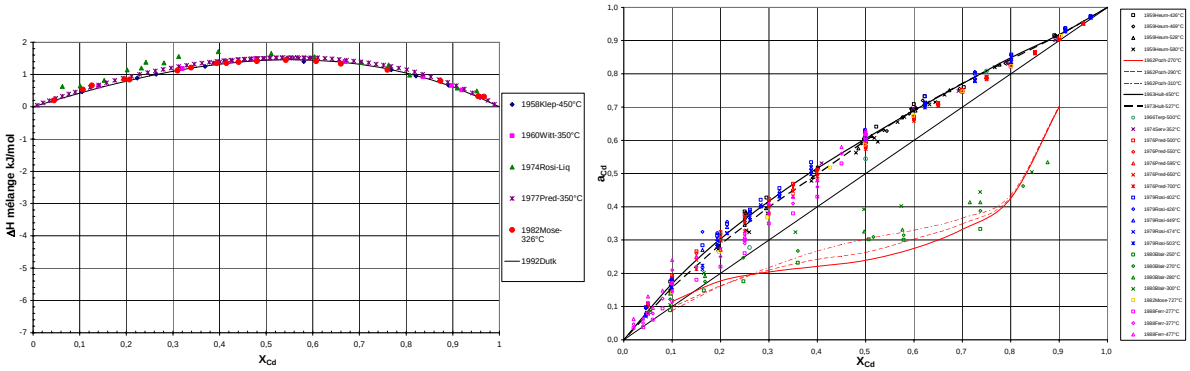

Figure 15 : (a) Mixing enthalpy of Cd-In alloy, (b) In activity in liquid Cd-In

D. CONCLUSIONS

This paper described the recent developments performed on the SIC control rod and absorber elements behaviour in severe accident conditions in the frame of SARNET SIC group. This work builds on the state of the art previously described which highlighted two main items for improvements. At first the behaviour of the rod at the time of its rupture must be better described. In this area the amount of Cd released at the rod rupture has also to be better characterized. Secondly, the expressions of vapour pressure for absorber elements must be improved, namely by more reliable data on the activity coefficients.

Regarding the first point, the QUENCH-13 test was performed at FZK, supported by analytical separate tests performed also by FZK on small specimens. QUENCH-13 was designed by careful pre-test calculations performed by PSI (SCDAP), EDF (MAAP4) and GRS (ATHLET-CD). Following the test conduct, analyses of the frozen melts were performed at FZK whereas reliable sampling and analyses of aerosols release during the test were performed by AEKI and PSI.

The analytical tests showed rod ruptures in the temperature range 1500-1630 K, thus always below the stainless steel melting temperature, and with very different modes of rupture from small failure with rivulets of molten materials to explosion of specimen. It is clear that Fe-Zr interactions played a major role in the rupture, confirmed by the rod rupture in QUENCH-13 occurring between 1550 and 1620 K. This confirms what was previously observed in [20] Accurate description of rod rupture thus needs rather complex descriptions of interactions (this is proposed in SCADP modelling) or at least for user defined rupture one needs to take into account of anticipated rupture by interactions (all the codes ATHLET-CD, MAAP4 and ASTEC allow the user to define such a criterion). Burst release of Cd vapour is clearly identified at the rod rupture from AEKI aerosol analyses (table 2) and PSI on-line aerosol measurements (fig 7). This needs calculation of the Cd vaporized in the rod prior its rupture. Just after the rod rupture Cd and In are the two main components of aerosols released (tables 2 and 3) whereas Ag release occurs rather late in the sequence. These results are consistent with analyses of frozen melt at middle elevation for which Cd content is very low whereas Zr (and Fe) content is very significant (table 1).

The review of thermodynamic data for the system Ag-In-Cd-Zr-H-O has began by the simple Ag-Cd; Ag-In; Cd-In binary systems showing that Cd activity experimentally deviates negatively from the ideal behavior in Ag-Cd and that indium activity experimentally deviates negatively from the ideal behavior in Ag-In system. There are no data related to activity or mixing enthalpy in the ternary system Ag-In-Cd in the liquid state and determinations activity or mixing enthalpy for compositions representative of the ternary alloys are envisaged to

complete the experimental database and to allow the modelling of the Gibbs energy of the ternary alloys in the liquid state. The ternary system is important because its vaporisation, prior the rod rupture produces a significant amount of Cd vapour which is immediately released at the rod rupture as shown by analyses of aerosols in the QUENCH-13 test. The present bibliographic work will continue with the higher order systems including zirconium (component of the guide tube) and gas constituents (hydrogen and oxygen). In the same time, post-test analyses will continue, supported by additional separate-effects tests and post-test calculations.

Acknowledgements

This work has been conducted under contract SARNET FI6O-CT-2004-509065.

References

[1] M. Schwarz, G. Hache, P. von der Hardt, “PHEBUS FP: A Severe Accident Research Programme for Current and Advanced Light Water Reactors”, Nucl. Eng. Des. 187 (1999) 47.
[2] L. Cantrel, E. Krausmann: “Reaction Kinetics of a fission-product mixture in a steam-hydrogen carrier gas in the PHEBUS primary circuit”, Nucl.Technol.144 (2003) 1-15.
[3] D.A. Petti, “Silver-Indium-Cadmium Control Rod Behavior and Aerosol Formation in Severe Reactor Accidents”, NUREG/CR–4876, April 1987.
[4] D.A. Petti, “Silver-Indium-Cadmium control rod behavior in Severe Reactor Accident” Nucl. Technol. 84 (1989) 128.
[5] H. Albrecht, "Freisetzung von Spalt- und Aktivierungsprodukten beim LWR-Kernschmelzen" - Abschlussbericht des SASCHA-Programmes", Kernforschungszentrum Karlsruhe, KfK 4264, June 1987.
[6] B.R. Bowsher et al., "Silver – Indium – Cadmium Control Rod Behaviour during a Severe Reactor Accident", Winfrith AEEW-R 1991, April 1986.
[7] A.M. Beard, P.J. Bennett, "Characterisation of Control Rod Release Rates and Aerosol Behaviour", AEA TRS 5064, March 1991.
[8] B. Rabu et al., "Silver- Indium-Cadmium- Tin Aerosol Releases and Control Rod Behaviour in PWR Accident Conditions", J. Aerosol Sci. Vol.30, Suppl.1, pp. S109-S110, 1999.
[9] S. Hagen, P. Hofmann, V. Noack, L. Sepold, G. Schanz, G. Schumacher, "Impact of Absorber Rod Material on Bundle Degradation Seen in CORA Experiments", Forschungszentrum Karlsruhe, FZKA 5680, December 1996.
[10] D.A. Williams, "OECD International Standard Problem Number 34 – FALCON Code Comparison Report" AEA Winfrith Technology Centre, AEA RS 3394, NEA/CSNI/R (1994)27, 1994.
[11] D.A.Petti, R.R. Hobbins, D.L. Hagrman, "The Composition of Aerosols Generated during a Severe Reactor Accident: Experimental Results from the Power Burst Facility Severe Fuel Damage Test 1-4", INEL (USA), Nuclear Technology vol.105, pp. 334-345, March 1994.
[12] B.Maliverney et al “Progress in Modelling Silver-Indium-Cadmium Control Rod Degradation and Release”, 1st European Review Meeting on Severe Accident Research (ERMSAR 2005), Aix en Provence, France, 14-16 November 2005.
[13] R.Dubourg “Minutes of the 3rd Meeting of the ST HITEMP Circle: Silver-Indium-Cadmium Behaviour”, Aix-en-Provence, 16 October 2006, SARNET-ST-M31.

[14] D.A. Powers, Sandia National Laboratories Report, IAEA–SM–281/35.
[15] T Haste, J Birchley, J-S Lamy, B Maliverney, H Austregesilo, C Bals, K Trambauer, M Steinbrück and J Stuckert, “Pre-Test Calculation Support for the QUENCH-13 Experiment”, Paper 8065 Proceedings of ICAPP ’08, Anaheim, CA USA, June 8-12, 2008.
[16] J. Stuckert et al, "First Results of the QUENCH-13 Bundle Experiment with a Silver-Indium-Cadmium Control Rod", Proc. 13th Int. QUENCH Workshop, 20-22 November 2007, Karlsruhe, Germany, ISBN 978-3-923704-63-7.
[17] J.Stuckert, “Some Results of EDX Analysis of Melt and Aerosols Released during the QUENCH-13 TEST”, Phebus Meeting, BIC circle, Bergen, 1-4 March 2008.
[18] R. Hillamo and E.I. Kauppinen, “On the Performance of the Berner Low Pressure Impactor”, Aerosol. Sci. Technol., 14 (1991) 33-47.
[19] Z. Hózer, P. Windberg, I. Nagy, L. Maróti, L. Matus, M. Horváth, A. Pintér, M. Balaskó, A. Czitrovszky, P. Jani: “Interaction of failed fuel rods under air ingress conditions”, Nucl. Technology, Vol. 141 (2003) 244-256.
[20] W.Hering, P.Hofmann, “Material Interactions during Severe LWR Accidents”, Technical report KfK 5125 (1995).